Cubic-tetragonal phase transition in $KMnF_3$: excess entropy and spontaneous strain

2000 J. Phys.: Condens. Matter 12 1133

(http://iopscience.iop.org/0953-8984/12/6/329)

J. Phys.: Condens. Matter **12** (2000) 1133–1142. Printed in the UK PII: S0953-8984(00)05617-4

Cubic–tetragonal phase transition in $KMnF_3$: excess entropy and spontaneous strain

S A Hayward†, F J Romero†, M C Gallardo†, J del Cerro†, A Gibaud‡ and E K H Salje§

† Departamento de Física de la Materia Condensada, Universidad de Sevilla, Apartado 1065, E-41080 Sevilla, Spain
‡ Laboratoire de Physique de l'Etat Condensé, Université du Maine, Avenue O Messiaen, 72085 Le Mans Cédex 9, France
§ Department of Earth Sciences, University of Cambridge, Downing Street, Cambridge CB2 3EQ, UK

E-mail: stuart@cica.es (S A Hayward)

Received 30 June 1999, in final form 28 October 1999

Abstract. The transition between cubic and tetragonal phases in $KMnF_3$ has been studied by x-ray diffraction rocking curves and calorimetry. Comparison of the excess entropy with the order parameter Q obtained from spontaneous strain shows that the mean field relationship $\Delta S \propto Q^2$ is obeyed to within experimental error. The data are fitted to a Landau free energy expression $\Delta G = \frac{1}{2}A(T - T_C)Q^2 + \frac{1}{4}BQ^4 + \frac{1}{6}CQ^6$, with $A = 2.781$ J K^{-1} mol^{-1}, $B = -57.63$ J mol^{-1}, $C = 574.2$ J mol^{-1}, $T_C = 185.76$ K. No significant excess specific heat is found at $T \gg T_C$.

1. Introduction

Materials with the perovskite structure (or one of its derivatives) occur in a wide range of natural and technological contexts (Navrotsky and Weidner 1989). The perovskite structure has a number of potential instabilities, which lead to a diversity of types of phase transition behaviour. The transitions in this family of materials have been extensively studied for two main reasons. One reason is their importance in a variety of applications. Another consideration is that, since the perovskite structure is so simple, these transitions provide a good test for theories of phase transitions. $SrTiO_3$ has been particularly important in this respect, as reviewed by Cowley (1996).

In geometrical terms, the $Pm3m$–$I4/mcm$ phase transition seen in $KMnF_3$ is identical to the transition in $SrTiO_3$. The transition involves the condensation of the R_{25} soft mode at the point [111] on the Brillouin zone boundary (Minkiewicz *et al* 1970). This mode is associated with the rotation of MnF_6 octahedra around the [001] axis. The primary order parameter is thus understood as the rotation angle of these octahedra; $Q \propto \phi$. In terms of the notation introduced by Glazer (1972), the tilt system for the transition is $a^0a^0c^-$.

The phase transition may be identified using a number of different experimental techniques. Early evidence for the transition (Beckman and Knox 1961, Okazaki and Suemune 1961) came from spontaneous strain measurements by standard x-ray diffraction methods. The strain is not large, and improved precision may be obtained by using 'high resolution/rocking curve' methods to measure the splitting between diffraction maxima of different twin domains (Nicholls and Cowley 1987, Cox *et al* 1988, Gibaud *et al* 1991, Burandt *et al* 1994). A set of superlattice reflections is associated with the $Pm3m$–$I4/mcm$ transition (Minkiewicz *et al* 1970), which

0953-8984/00/061133+10$30.00

may be used to distinguish the structures of the phases. The use of the intensity of these satellite reflections to measure the order parameter is more problematic (Burandt *et al* 1994), since the domain microstructure in tetragonal $KMnF_3$ is highly variable, even within a single experiment (Tietze *et al* 1981, Hirakawa *et al* 1997). Experimental data also exist from ultrasonic studies of the soft mode (Furukawa *et al* 1970), and Raman spectroscopy (Kapusta *et al* 1999).

From these studies, it is apparent that the cubic–tetragonal transition in $KMnF_3$ is first order, though the size of the first order step is not large. Most authors fit their data for the order parameter to a power law of the form $Q \propto |T_C - T|^{\beta}$, and obtain β values in the range 0.25–0.32. As Burandt *et al* (1994) note, this uncertainty is, at least in part, due to the mathematical difficulty of fitting data for a discontinuous transition to a continuous power law.

Although the crystallographic aspects of the transition are well understood, a complete thermodynamic description of the experimental data has been more elusive. Two distinct approaches may be identified, emphasizing the role of critical fluctuations and the mean field respectively.

The universality class of the $Pm3m$–$I4/mcm$ transition in both $SrTiO_3$ and $KMnF_3$ corresponds to a Hamiltonian of a 3D Heisenberg type with a cubic anisotropic part of the soft modes and their dispersion. The critical exponents for the isotropic $n = 3$, $d = 3$ fixed point were calculated by le Guillou and Zinn-Justin (1980) as $\beta = 0.365$, $\gamma = 1.386$.

Even for strong cubic anisotropy the Heisenberg fixed point remains stable (Bruce and Aharony 1975), but for large dispersion forces the transition becomes first order as the Heisenberg fixed point is not accessible (Nattermann 1976, Rudnick 1978). According to this argument, the difference between the continuous transition observed in $SrTiO_3$ and the first order transition of $KMnF_3$ is the strength of the cubic anisotropy. Müller and Berlinger (1982) argued in addition that weak fields (e.g. external stresses along [111]) may change the transition completely yielding Ising and Potts transitions.

The alternative approach to the theoretical description of the transition is to use a mean field model, such as Landau theory. Recent studies of $SrTiO_3$ (Salje *et al* 1998, Hayward and Salje 1999) have shown that the various experimental data for the transition are selfconsistently described by a Landau potential. Based on this work, the temperature range over which criticalities may be observed is less than 1 K. In the case of $KMnF_3$, Stokka *et al* (1981) used Landau theory to analyse the results of a calorimetric experiment, though these authors did not calculate all the coefficients of the potential. The variation of the order parameter with pressure in $KMnF_3$ was studied by Åsbrink and Waskowska (1996), who also interpreted the data with Landau theory.

In this study, we perform calorimetric measurements (latent heat and specific heat) and high resolution x-ray measurements of the spontaneous strain on a single sample of $KMnF_3$. Comparison of the spontaneous strain with the latent heat and specific heat is used to confirm that the strain and the excess entropy are related in the way predicted by a mean field model, and to determine the coefficients of a Landau potential. The significance of our results is that we show that both model transitions in the perovskite structure, namely high purity $SrTiO_3$ and $KMnF_3$, follow mean field behaviour with minimal, if any deviations which can clearly be related to criticalities outside the mean field limit.

2. Experimental methods

2.1. Sample synthesis

The sample was prepared using the Bridgmann–Stockbarger method. The resulting crystal was approximately cylindrical, with a thickness of 5 mm and circular (001) faces with area 0.8 cm^2.

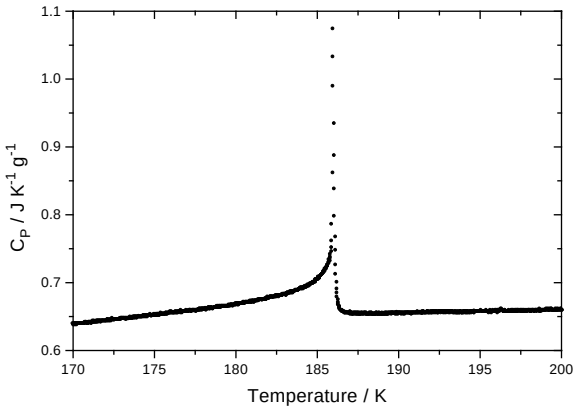

Figure 1. Temperature dependence of the specific heat in a pure $KMnF_3$ single crystal in the vicinity of the cubic–tetragonal phase transition.

2.2. Calorimetric measurements

The measurements of latent heat and specific heat were performed on a high resolution conduction calorimeter, which has been described in detail elsewhere (Gallardo *et al* 1995). The apparatus consists of two identical heat fluxmeters, each consisting of 50 chromel–constantan thermocouples connected in series with wires arranged in parallel lines. Two electrical resistance heaters are used in the system, one situated between each face of the sample and the fluxmeters. These heaters dissipate a uniform heat on the sample faces or measure the temperature of the fluxmeter junctions near the sample. The other ends of the fluxmeters are pressed against a 10 kg bronze cylinder, which acts as a heat sink. This calorimeter block is suspended within a cylindrical radiation shield, and the whole assembly is then placed in a hermetic outer case, within which a high vacuum (10^{-5} Pa) may be produced. The system is then surrounded by a coiled tube, and placed in an alcohol bath. Liquid N_2 circulates through the coil, and regulates the temperature of the alcohol bath. The large number of thermocouples used, together with the good thermal stability (due to the system's large thermal inertia), allow very small temperature changes to be studied in a stable manner. As a result, it is possible to change the sample temperature extremely slowly without inducing temperature fluctuations in the block—a heating or cooling rate of 0.06 K h^{-1} is quite achievable.

It is also important to note that the system produces two sets of results—the heat flux and the specific heat. As a result, the specific heat and any latent heat can be determined independently, but under similar thermal conditions (del Cerro *et al* 2000).

The specific heat is measured by starting from the steady state obtained when the same power is dissipated by both resistances. This heat power W crosses through the fluxmeter, producing an electromotive force V in the fluxmeter. The power is then cut off (at a time t_0), and V is integrated up to the time t_1 when equilibrium is reached again. The specific heat C is proportional to the integral of V with respect to t between t_0 and t_1. The increase in the sample temperature in this measurement process is of the order of 0.06 K. Figure 1 shows the variation of the specific heat of $KMnF_3$ in the temperature range between 170 K and 200 K.

The latent heat of the transition is measured by heating or cooling the calorimeter at a constant rate without dissipation in the heaters, and recording the electromotive force $V(t)$ in the fluxmeters. The e.m.f. is proportional to heat flux ϕ, the integral of which is in turn proportional to the excess enthalpy of the sample.

The heat flux can have two contributions: one due to the latent heat and another due to the variation of specific heat with temperature. In an idealized first order transition, the latent heat would appear as a spike in the $\phi(t)$ graph, which would be trivial to separate from the specific

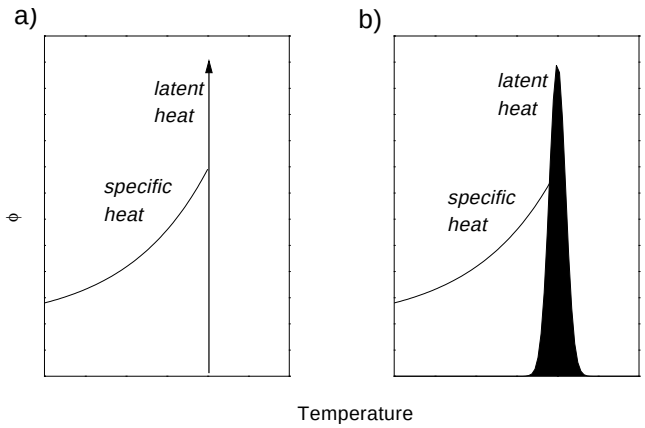

Figure 2. The problem of separating contributions from latent heat and specific heat in the heat flux. (a) The idealized situation is that the transition occurs at a single temperature T_{TR}. In this case, the latent heat appears as a sharp spike in the $\phi(T)$ graph, and is easy to separate from the specific heat. (b) In a real experiment, the transition is somewhat smeared in the temperature axis. As a result, there is a temperature range where the specific heat and latent heat overlap. The resolution of these two effects creates some ambiguity in the analysis of the calorimetric data for first order transitions.

heat (figure 2(a)). In reality, the transition occurs over a range of temperatures, with lower and upper limits T_- and T_+. Consequently, the latent heat is smeared out, and so overlaps with the specific heat contribution (figure 2(b)). This problem is particularly significant in $KMnF_3$, since the latent heat is not large, and the specific heat shows a strong anomaly close to the transition.

del Cerro *et al* (2000) show that this ambiguity may be overcome, provided independent but consistent measurements of the specific heat and heat flux exist. From the specific heat data (figure 1), we determine the part of the heat flux due to the specific heat contribution, ϕ_C. Within the two-phase region, the temperature dependence of ϕ_C will be complicated by the presence of two phases in the sample. As C and ϕ are measured on a single sample under the same thermal conditions, ϕ and ϕ_C may be compared directly. The latent heat occurs in the temperature range T_- to T_+, where ϕ and ϕ_C do not coincide, which is thus the two-phase field for the transition. Figure 3(a) shows ϕ and ϕ_C as a function of temperature for $KMnF_3$ being heated and cooled through the transition. Figure 3(b) shows the part of the heat flux due exclusively to the latent heat. The area under this curve gives the latent heat associated with the transition.

2.3. X-ray diffraction experiments

The spontaneous strain associated with the phase transition was measured using x-ray rocking experiments, using a similar method to that used by Chrosch and Salje (1998) to study $SrTiO_3$. The sample was mounted on a high resolution, two-circle diffractometer ('X1' in Locherer *et al* 1996) fitted with a cryostat. The splitting of the strong 200 reflection was measured as a function of temperature between 190 K and 90 K, with (001) as the basal plane and [010] as the rocking axis (all orientations relative to the cubic crystal axes). Rocking curves were collected every 5 K for both heating and cooling. Monochromatic Cu Kα_1 radiation was used for the incident x-ray beam, with a small beam width ($\sim$0.2 mm) to minimize beam divergence. The step size in the rocking angle ω was 0.01°. At each ω position, the intensity–2θ spectrum was recorded, and the total intensity in the 200 peak ($2\theta \approx 43.25°$) was determined by integration. The rocking curve is the manifestation in reciprocal space of the twin microstructure; each

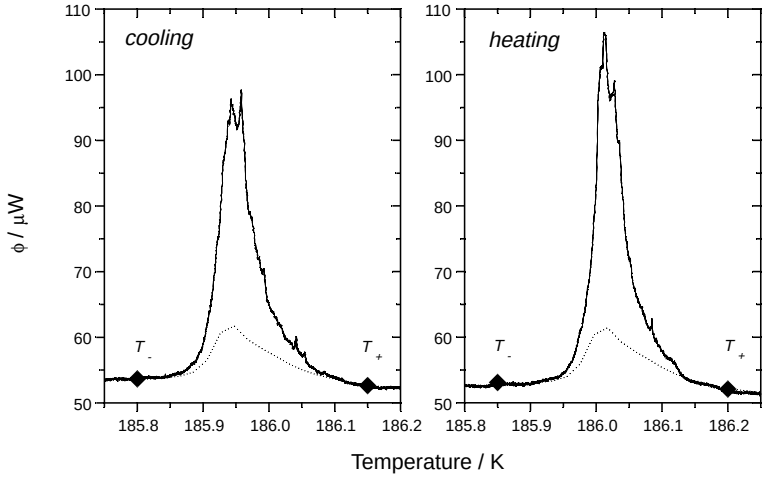

(a)

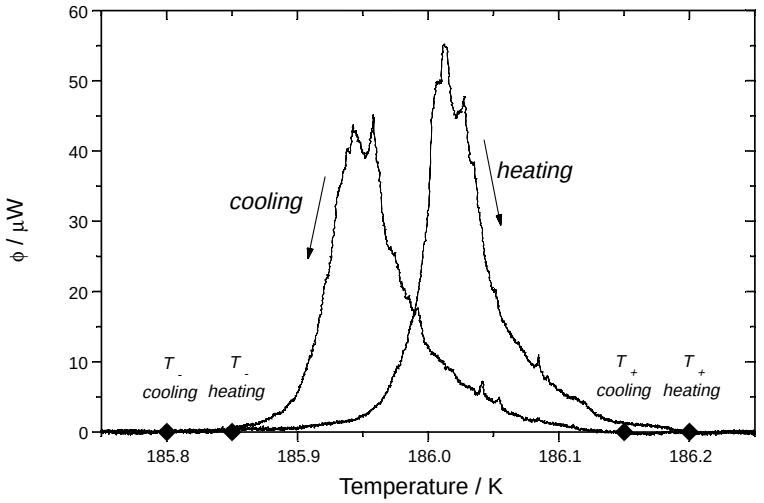

(b)

Figure 3. (a) Variation of heat flux (ϕ solid line) with temperature as $KMnF_3$ is heated and cooled through the cubic–tetragonal phase transition, and the component due to specific heat (ϕ_C, broken line). The upper and lower limits of the temperature range where ϕ and ϕ_C do not coincide are marked as T_+ and T_- respectively. (b) Component of heat flux due to latent heat. The areas under the two curves are proportional to the latent heats observed on heating and cooling, and are equal.

peak represents a distinct twin domain; the $\Delta\omega$ between rocking peaks is the twin angle which increases with the spontaneous strain.

For the experimental configuration used here, four distinct twin domain orientations can be observed on tilting around the ω axis. Taking the splitting between the highest and lowest ω peaks, we obtain a twin angle $\Delta\omega$ as a function of temperature. This twin angle is related to the ratio of the pseudo-cubic lattice parameters by $\Delta\omega \propto (c/a) - 1$. Thus the rocking experiment determines the difference of the spontaneous strains $e_3 - e_1$. This function is proportional to the symmetry-adapted strain e_t of Carpenter *et al* (1998), and scales as the square of the order

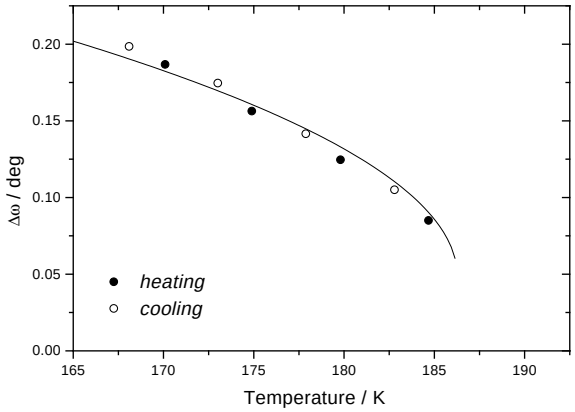

Figure 4. Twin angle, proportional to the square of the order parameter, as a function of temperature in pure $KMnF_3$. The solid line shows the predictions of a model derived exclusively from calorimetric measurements, as discussed in section 4.4.

parameter Q^2. The twin angle is plotted as a function of temperature in figure 4.

3. Application of Landau theory to first order transitions

From the generic classical Landau potential

$$\Delta G = \frac{A}{2}(T - T_C)Q^2 + \frac{B}{4}Q^4 + \frac{C}{6}Q^6 \tag{1}$$

the temperature dependence of the square of the order parameter is given by

$$Q^2 = \frac{-B + \sqrt{B^2 + 4AC(T_C - T)}}{2C}. \tag{2}$$

For a first order transition, it is convenient to express equation (2) as a function of the equilibrium transition temperature T_{TR};

$$Q^2 = \frac{2}{3}Q_0^2\left\{1 + \left[1 - \frac{3(T - T_C)}{4(T_{TR} - T_C)}\right]^{1/2}\right\} \tag{3}$$

where Q_0 is the step in the order parameter at T_{TR};

$$Q_0^2 = \frac{4A(T_C - T_{TR})}{B} \tag{4}$$

$$T_{TR} - T_C = \frac{3B^2}{16AC}. \tag{5}$$

The magnitude of the parameter A describes the scaling between the order parameter and the excess entropy;

$$\Delta S = -\frac{AQ^2}{2}. \tag{6}$$

Equation (3) can be re-written to describe the temperature dependence of the excess entropy;

$$\Delta S = \frac{2L}{3T_{TR}}\left\{1 + \left[1 - \frac{3(T - T_C)}{4(T_{TR} - T_C)}\right]^{1/2}\right\}. \tag{7}$$

An alternative way of using the specific heat data is to use equation (2) above, noting that $\Delta C = T(\partial \Delta S/\partial T)$. From this, it can be shown that

$$\left(\frac{T}{\Delta C_P}\right)^2 = \frac{4B^2 + 16AC(T_C - T)}{A^4}. \tag{8}$$

In a first order phase transition, there are three distinct temperatures which may be regarded (in some sense) as characteristic of the transition. The lowest of these is described as T_C in the above equations; this is the lowest temperature for which $Q = 0$ is a minimum in G, rather than a maximum. T_{TR} is the temperature at which G for the ferrophase and paraphase are equal, and so is the temperature at which an equilibrium transformation should occur. The highest characteristic temperature is T_2, which is the highest temperature for which the ferrophase may exist. Thus the extent of the two phase region on the phase diagram will be $T_C \leqslant T \leqslant T_2$. (In a thermodynamically second order transition, these temperatures of these three conditions coincide.) In a first order transition, T_2 is related to the other parameters by

$$T_2 - T_C = \frac{B^2}{4AC} \qquad T_2 - T_{TR} = \frac{3B^2}{16AC}. \tag{9}$$

Thus equation (7) may also be expressed as

$$\Delta S = \frac{2L}{3T_{TR}}\left\{1 + \left[1 + \frac{(T_2 - T)}{(T_2 - T_C)}\right]^{1/2}\right\} \tag{10}$$

and equation (8) as

$$\left(\frac{T}{\Delta C_P}\right)^2 = \frac{16C(T_2 - T)}{A^3} \tag{11}$$

or, differentiating (10),

$$\left(\frac{T}{\Delta C_P}\right)^2 = \frac{9d(T_2 - d/4)^2}{L^2}(T_2 - T) \tag{12}$$

where $d = T_2 - T_C$.

The coefficients of the Landau potential are completely determined by L, T_2 and d. L is measured in the heat flux experiment, T_2 is the temperature at which ΔC_P extrapolates to infinity, so d is fixed from the gradient of $(T/\Delta C_P)^2$ against T, as in equation (12).

4. Data analysis

4.1. Specific heat data

The most reliable data are those for the specific heat anomaly just below T_C. Here the magnitude of ΔC_P is large, and the error in the baseline is relatively small. Figure 5 tests the validity of equation (8) above, making the initial assumption that the baseline C_{P0} is a linear extrapolation of the specific heat at high temperatures. The function $(T/\Delta C_P)^2$ is found to be linear with temperature up to 185.75 K. As figure 3 above shows, this is the temperature where the influence of latent heat begins to affect experimental measurements of the specific heat.

The baseline C_{P0} is expected to display some downward curvature at low temperatures, though it is notoriously difficult to predict the exact form of this curve with enough precision to obtain accurate values for $\Delta C_P = C_P - C_{P0}$. In figure 6, we assume that $(T/\Delta C_P)^2$ remains linear with temperature, and calculate the form of the baseline consistent with this assumption. The final baseline is close to the Einstein curve for the phonon spectrum of $KMnF_3$. However, it is not possible to model the baseline exactly using the simplest forms of the Einstein or Debye models.

From the analysis of the heat flux curves by del Cerro *et al* (2000), as summarized in figures 3(a) and 3(b), the latent heat L has been determined as 0.129(2) J g^{-1}. When the sample is cooled at 0.06 K h^{-1}, the coexistence region for the paraphase and ferrophase extends from $T_+ = 186.15$ K to $T_- = 185.80$ K. On heating at the same rate, the coexistence region is from $T_- = 185.85$ K to $T_+ = 186.20$ K.

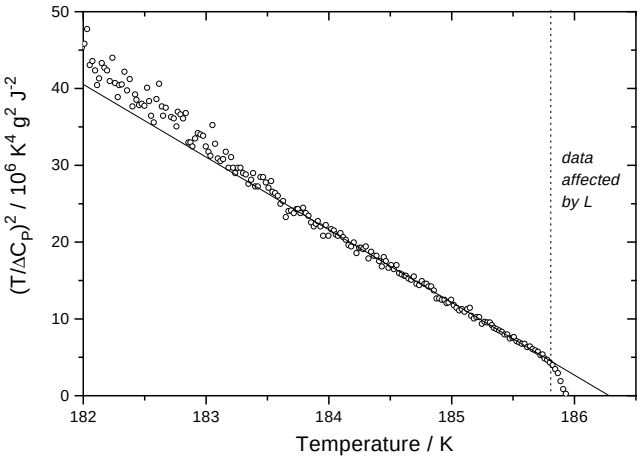

Figure 5. Temperature dependence of $(T/\Delta C_P)^2$ for $KMnF_3$ in the vicinity of the cubic–tetragonal phase transition. The linearity of this function is consistent with Landau theory. The deviations below ∼183 K probably arise from the inaccuracy of a linear extrapolation as a determination of the baseline function. The extrapolation of $(T/\Delta C_P)^2$ to zero gives $T_2 = 186.28$ K.

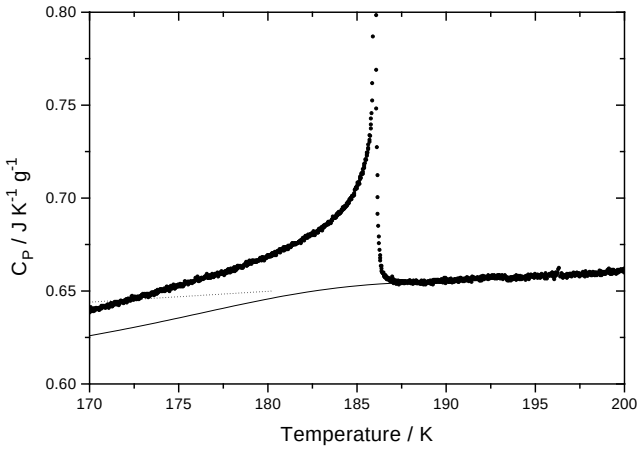

Figure 6. Temperature dependence of specific heat in $KMnF_3$, showing two possible baselines. A simple linear extrapolation of the data from above the transition (broken line) is of limited use, since it eventually crosses the experimental C_P curve. One way of determining the curvature of the baseline is to force ΔC_P to be consistent with some theoretical model. This is done here for a Landau model of the transition (solid line). Immediately below the transition, the difference between these two methods is negligible.

4.2. Comparison of entropy and spontaneous strain

Given the latent heat, and the variation of the excess specific heat with temperature, the temperature dependence of the excess entropy is calculated. Since this is proportional to Q^2 in a Landau model, this is then compared with the independently measured spontaneous strain e_t (also proportional to Q^2 in this transition). Figure 7 shows that the quantities ΔS and e_t are indeed proportional over a wide temperature range.

We may compare this result with the predictions of a criticality model, such as the 3D Heisenberg model (Le Guillou and Zinn-Justin 1980). If the excess specific heat varies as $|T_C - T|^{-\alpha}$, then the excess entropy will vary as $|T_C - T|^{1-\alpha}$. Meanwhile, the order parameter is expected to vary as $|T_C - T|^{\beta}$. For the 3D Heisenberg ($\alpha = -0.12$, $\beta = 0.365$) model, the excess entropy is expected to increase more rapidly with $|T_C - T|$ than the square of the order

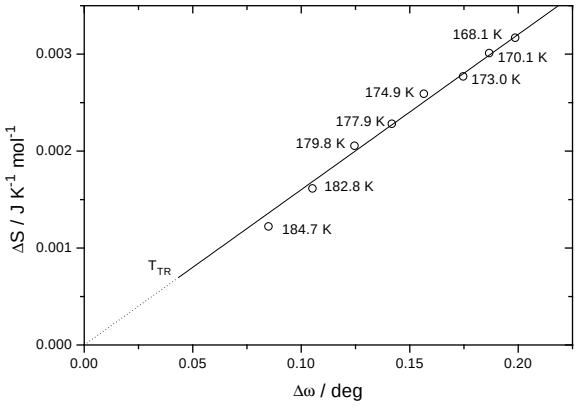

Figure 7. Comparison of excess entropy (calculated from latent heat together with extrapolated specific heat) and twin angle associated with the cubic–tetragonal phase transition in $KMnF_3$. The observed proportionality is consistent with a Landau treatment of the transition.

parameter. These values are not compatible with our experimental observations.

4.3. Calculation of Landau coefficients

We now calculate the coefficients for a Landau potential for $KMnF_3$. From the heat capacity data, we note that $T_2 = 186.28(1)$ K, and that the gradient of the $(T/\Delta C_P)^2$–T line is $-9.465(5) \times 10^6$ K^3 g^2 J^{-2}. Note that neither of these quantities depends much on (reasonable) choices of the baseline. From the heat flux data, we know that $L = 0.129(2)$ J g^{-1} (del Cerro *et al* 2000). Determination of T_{TR} is more ambiguous. When the sample is cooled, we expect $T_{TR} = T_+$, which in this case is 186.15(1) K. For heating, we expect $T_{TR} = T_-$, or 185.85(1) K. Clearly, these quantities do not agree. However, since only three data are needed to constrain the 2:4:6 Landau potential, the exact value of T_{TR} can be ignored at this stage.

Given the experimental values for L, T_2, and the gradient of the $(T/\Delta C_P)^2$–T line, we obtain $T_2 - T_C = 0.52$ K. Hence, $T_C = 185.76$ K and $T_{TR} = 186.15$ K, in good agreement with the analysis of the heat flux data for cooling (though not for heating).

To find the Landau coefficient A, we extrapolate either equation (7) or equation (10) to $T = 0$ K. Using this, we find $\Delta S(0\,\mathrm{K}) = 9.21 \times 10^{-3}\,\mathrm{J\,K^{-1}\,g^{-1}}$. Hence $A = 0.0184\,\mathrm{J\,K^{-1}\,g^{-1}}$. Substituting L and T_{TR} into equations (4) and (5), we obtain $B = -0.3816$ J g^{-1}, $C = 3.801$ J g^{-1}. The equivalent molar quantities, given 1 mol $KMnF_3 = 151.04$ g, are $A = 2.781$ J K^{-1} mol^{-1}, $B = -57.63$ J mol^{-1}, $C = 574.2$ J mol^{-1}. As a final illustration of the model, the fit line in figure 4 shows the temperature dependence of the order parameter predicted by the model determined from the calorimetric data. This agrees well with the experimental data for the twin angle (i.e. the spontaneous strain).

5. Discussion

In this study, we have shown that the temperature dependence of both the excess entropy and the spontaneous strain may be described consistently in terms of a single Landau model. This result is consistent with earlier analyses of $SrTiO_3$ (Salje *et al* 1998, Hayward and Salje 1999), but not with the description of this transition in terms of criticality models. There are no obvious deviations from mean field behaviour in the x-ray data (which includes data up to $T_C - 2$ K), or in the heat capacity data (which includes data up to within 0.1 K of T_C). Significantly, the spontaneous strain is found to be proportional to the excess entropy, which is a characteristic result of Landau theory.

In addition, the temperatures T_C and T_{TR} correlate remarkably well with the lim-

its of the coexistence interval for cooling of the sample ($T_C = T_- = 185.8$ K, and $T_{TR} = T_+ = 186.15$ K). When heating the sample, the transition starts somewhat before T_{TR} is reached ($T_- = 185.85$ K). The reason for this is not entirely clear. It is possible that non-equilibrium defects and microstructures in the tetragonal phase reduced the stability of this phase with respect to the cubic phase in this experiment, and so promoted the tetragonal–cubic transition on heating. There is no measurable difference in the excess entropy between heating and cooling, and so any such effect must be small. However, the ΔG between the two phases near T_C is also small, so defect effects may explain difference between the observed value of T_- (185.85 K) and the expected value (186.15 K) in the heating experiment.

In figure 5, we noted that the specific heat data just between T_C and 187.75 K deviated from the linear predictions of Landau theory. This is an experimental problem, related to the onset of latent heat associated with the first order transition. The temperature above which this effect occurs correlates well with T_C, which is the lowest temperature at which a (non-equilibrium) transition is possible. No further excess specific heat was found at higher temperatures.

Acknowledgments

This project is part of the EU TMR network 'Mineral Transformations' (ERB-FMRX-CT97-0108), and is also supported by the Spanish DGICYT (PB95-0546), and the British–Spanish Joint Research Programme HB 1997-0180.

References

Åsbrink S and Waskowska A 1996 *Phys. Rev.* B **53** 12
Beckman O and Knox K 1961 *Phys. Rev.* **121** 376
Bruce A D and Aharony A 1975 *Phys. Rev.* B **11** 478
Burandt B, Rothaug S and Press W 1994 *J. Phys.: Condens. Matter* **6** 7189
Carpenter M A, Salje E K H and Graeme-Barber A 1998 *Eur. J. Mineral.* **10** 621
Chrosch J and Salje E K H 1998 *J. Phys.: Condens. Matter* **10** 2817
Cowley R A 1996 *Phil. Trans. R. Soc.* A **354** 2799
Cox U J, Gibaud A and Cowley R A 1988 *Phys. Rev. Lett.* **61** 982
del Cerro J, Romero F J, Gallardo M C, Hayward S A and Jiménez J 2000 *Thermochim. Acta* **343** 89
Furukawa M, Fujimori Y and Hirakawa K 1970 *J. Phys. Soc. Japan* **29** 1528
Gallardo M C, Jiménez J and del Cerro J 1995 *Rev. Sci. Instrum.* **66** 5288
Gibaud A, Shapiro S M, Nouet J and You H 1991 *Phys. Rev.* B **44** 2437
Glazer A M 1972 *Acta Crystallogr.* B **28** 3384
Hayward S A and Salje E K H 1999 *Phase Transitions* **68** 501
Hirakawa K, Lu ZL, Soejima Y and Okazaki A 1997 *Phase Transitions* **60** 131
Kapusta J, Daniel P and Ratuszna A 1999 *Phys. Rev.* B **59** 14 235
le Guillou J C and Zinn-Justin J 1980 *Phys. Rev.* B **21** 3976
Locherer K R, Hayward S A, Hirst P J, Chrosch J, Yeadon M, Abell J S and Salje E K H 1996 *Phil. Trans. R. Soc.* A **354** 2815
Minkiewicz V J, Fujii Y and Yamada Y 1970 *J. Phys. Soc. Japan* **28** 443
Müller K A and Berlinger W 1982 *Z. Phys.* B **46** 81
Nattermann T 1976 *J. Phys. C: Solid State Phys.* **9** 3337
Navrotsky A and Weidner D (eds) 1989 *Perovskite: a Structure of Great Interest to Geophysics and Materials Science* (Washington: American Geophysical Union)
Nicholls U J and Cowley R A 1987 *J. Phys. C: Solid State Phys.* **20** 3417
Okazaki A and Suemune Y 1961 *J. Phys. Soc. Japan* **16** 671
Rudnick J 1978 *Phys. Rev.* B **18** 1406
Salje E K H, Gallardo M C, Jiménez J, Romero F J and del Cerro J 1998 *J. Phys.: Condens. Matter* **10** 5535
Stokka S, Fossheim K and Samulionis V 1981 *Phys. Rev. Lett.* **47** 1740
Tietze H, Müllner M and Jex H 1981 *Phys. Status Solidi* a **66** 239